Hindawi
International Journal of Corrosion
Volume 2024, Article ID 5577674, 8 pages
https://doi.org/10.1155/2024/5577674

Research Article

Empirical Study of the Effect of Nanocoolant Particles on Corrosion Rate of 316 Stainless Steel

Yuli Panca Asmara,[1] **Jeya gopi Raman**,[1] **Suparjo**,[2] **Firda Herlina**,[3] **and Yap Chun Wei**[4]

[1]*INTI International University, Faculty of Engineering and Quantity Surveying, Nilai 71800, Negeri Sembilan, Malaysia*
[2]*Engineering Faculty, University of Mataram, Mataram, West Nusa Tenggara, Indonesia*
[3]*Universitas Islam Kalimantan Muhammad Arsyad Al Banjari Banjarmasin, Banjarmasin, Indonesia*
[4]*Student of Mechanical Engineering, UMP, Pekan, Malaysia*

Correspondence should be addressed to Yuli Panca Asmara; ypanca@hotmail.com

Received 14 August 2023; Revised 15 March 2024; Accepted 4 April 2024; Published 6 May 2024

Academic Editor: Manikandan M

The advancement of nanotechnology has had an impact on the use of heat exchangers. Nanocoolants, which offer higher thermal efficiency than traditional coolants, have paid significant attention. These innovative fluids, which contain nanomaterials, not only have better heat efficiency but also improve energy efficiency compared to regular coolants. However, the presence of solid nanoparticles in the coolant may cause corrosion and erosion of tubes, leading to massive degradation of those parts. To evaluate the effectiveness of nanocoolant particles, this research was conducted by studying the impact of using nanocoolant on erosion-corrosion occurring on metal surfaces. The study focused on the erosion-corrosion of stainless steel (AISI 316) in coolant solutions containing nanoparticles. The experiments utilized a rotating cylinder electrode (RCE) with rotational speeds ranging from 0 to 1800 rpm and a temperature range of 30°C-70°C. The corrosion rate was determined using the linear polarization resistance (LPR) method, while the erosion was measured by calculating the average surface roughness of the samples. The design of the experiment (DOE) was utilized to find the mathematical expressions of the effects of the nanocoolant on erosion and corrosion. The findings revealed that the corrosion rate and surface roughness of the samples increased with an increase in temperature and rotation speed. Furthermore, the erosion-corrosion effects of the nanocoolant were less significant in stagnant conditions than in flow conditions, and significant differences were observed when compared with conventional coolant. Additionally, synergistic erosion and corrosion processes were detected at higher temperatures and higher rotation speeds for both types of coolants.

1. Introduction

The cooling mechanism within a heat exchanger has significant importance in industrial uses. Engineering processes that involve high-speed and high-power engines necessitate a dependable cooling system to maintain stable operational temperatures. The heat exchanger is a device to transfer heat between one or more fluids. In the heat exchanger, the fluid is separated by a solid wall to prevent mixing or direct contact. Shell and tube heat exchangers consist of a series of metallic tube bundles which contain fluids to provide or absorb heat. This design is designed for higher-pressure applications and low corrosion rates. Oil, water, and various other synthetic liquids are typical substances used in cooling systems, yet their effectiveness in heat transfer is constrained.

Corrosion is among the general failure modes that occur in metallic structures including heat exchangers [1, 2]. Corrosion erosion is one of the factors that can not only cause damage to equipment but also cause malfunction of equipment, especially in piping systems [3–9]. The rate of deterioration is affected by the type of material, manufacturing process, shape, and geometry, as well as the corrosive environment. Surface conditions also play a role in influencing the resistance of objects to corrosion [5, 10–12]. During

the corrosion process, metal loss occurs due to electrochemical reactions on the surface which can cause various types of corrosion, especially pitting, intergranular, or transgranular corrosion [1, 13–15]. The metal degradation due to corrosion is further accelerated in the presence of solid particles, which contribute to wear and erosion impacts. Extensive experimental work has established a correlation between surface roughness (Rz) and the corrosion process [14, 16, 17]. Stoilov and Northwood [12] created varied levels of surface roughness on nickel surfaces using SiC papers, subsequently comparing their corrosion properties. Evaluations through techniques such as electrochemical impedance spectroscopy (EIS) and profilometry revealed that lower roughness values were correlated with elevated corrosion resistance. Additionally, the effect of surface roughness on the corrosion process was also observed by Hong and Nagumo [11]. They proved that rougher surfaces initiate the early stages of pitting corrosion in type 301 stainless steel. Other works conducted by Zhao et al. [18] further revealed that the roughness of the metallic surface significantly influences the corrosion resistance of sol-gel coatings on AA2024 alloys.

Traditional cooling mediums, such as water or ethylene glycol, have limitations in terms of uniformity in thermal conductivity, thermal stability, and heat capacity, as well as requiring more area for heat exchange, resulting in impractical power consumption, particularly in high-performance heat transfer applications [2]. However, nanofluids, composed of nanoparticles dispersed in base fluids like ethylene glycol and water, offer improved thermal conductivity and stability compared to traditional cooling agents [4, 19, 20]. Research shows that nanofluids provide heightened conductivity and enhanced thermal stability, making them a promising alternative for various heat transfer applications [21–23]. Nonetheless, utilizing nanofluids in cooling systems presents challenges, as solid particles within the fluid can lead to corrosion and erosion of pipe surfaces, raising concerns about the impact of nanocoolants on metal degradation rates [24–29]. Recent studies have explored methods to mitigate these issues, such as using image processing to assess surface roughness and investigating the addition of graphene nanoparticles to improve corrosion resistance [30]. In 2019, Wang et al. [31] investigated how adding graphene nanoparticles to nanofluids improved the corrosion resistance of carbon steel. They found that the presence of graphene led to better corrosion resistance than the base fluid alone. Similarly, Li et al. [32] studied the erosion-corrosion behavior of stainless steel in nanocoolants containing silica nanoparticles. Computational modeling techniques, like molecular dynamics simulations, are also being used to predict the performance of steel in nanocoolant environments [33]. Overall, while nanofluids offer significant advantages, addressing their potential drawbacks is essential for their effective implementation in cooling systems. By studying the risks associated with nanoparticles in coolants and comparing them with traditional cooling methods, it can enhance the understanding of the reliability of cooling systems. This, in turn, paves the way for the development of improved technologies that prioritize sustainability and efficiency.

Table 1: Chemical properties of TiO_2.

Chemical data	
Symbol	TiO_2
CAS no.	1317-80-2
Group	Titanium 4 Oxygen 16
Chemical composition	
Content of elements	(%)
Titanium	59.93
Oxygen	40.55

Table 2: Physical properties of TiO_2.

Properties	Metric	Imperial
Density	4.2 g/cm^3	0.15 lb/in^3
Molar mass	79.9	

Table 3: Thermal properties of TiO_2.

Properties	Metric	Imperial
Melting point	184°C	335°F
Boiling point	297°C	538°F

Table 4: Mechanical properties of stainless steel AISI 316.

Tensile strength (MPa)	59
Yield strength (MPa)	272
Hardness (HV)	82

2. Experimental Setup

2.1. Nanoparticles Materials. Titanium dioxide exists in the form of nanocrystals or nanodots, characterized by their substantial surface area. This compound is also recognized by various names, including flamenco, rutile, titanium oxide, and dioxotitanium. The chemical, physical, and thermal attributes are presented in Tables 1–3.

The nanofluid is prepared by introducing titanium dioxide (TiO_2) nanoparticles at a concentration of 1% by volume into the ethylene glycol-based fluid (EG). The mixture is stirred continuously for several hours to attain a uniformly distributed solution. It is noted that EG, enhancing film formation, has an impact on the reduction of corrosion rates [20]. However, this experiment specifically focuses on EG with a fixed concentration of 1%. The chemicals used were from UMP, Malaysia.

2.2. Material Tested. The materials used were stainless steel 316. The austenitic structure of stainless steel 316 gives excellent toughness, even at cryogenic temperatures. The mechanical properties of AISI 316 are presented in Table 4. Figure 1 shows the samples employed for studying the corrosion rate under various flow rate conditions. The 316 stainless steel samples were from UTP, Malaysia.

Figure 1: Stainless steel AISI 316 specimen.

Table 5: Electrodes for LPR.

Electrode	Example
The working electrode (WE)	SS-AISI316
The reference electrode (RE)	Saturated calomel electrode (SCE): reference electrode based on the reaction between elemental mercury and mercury (I) chloride
The counter electrode (CE)	Carbon electrodes

2.3. Corrosion Test

2.3.1. Linear Polarization Resistance (LPR) Method. LPR, or linear polarization resistance, is a method that involves applying a small electrical current to the metal surface, inducing a potential difference. This method measures the rate of corrosion by recording the potential and current passing through the metal surfaces. The corrosion rate data were obtained using the Wonatech WPG100e Potentiostat/Galvanostat, Korea. The hotplate used was from Labtech, Daihan Scientific, Korea, while the overhead stirrer was from Wisestir, UK. For all tests conducted, graphite rods and Ag/AgCl electrodes from Gamry, UK, were selected as the reference electrodes. Table 5 shows the electrodes utilized to measure the corrosion rate using the LPR method.

2.3.2. Surface Roughness Tester. A surface roughness tester is used to calculate the roughness average (R_a). Roughness (R_a) measures an average of the absolute values of the roughness profile surfaces. Surface roughness was measured using contact profilometers, which physically trace the surface with a stylus to measure its profile (UMP Lab, Malaysia).

Table 6: Experimental parameters.

Temperature (°C)	30, 40, 50, 60, & 70
Rotational speed (rpm)	0, 300, 700, 1100, 1500, & 1800
Coolant	Nanocoolant

Table 7: Original and coded variables.

Level	Code	Rotational speed (rpm)	Temperature (°C)
Axial point	$\sqrt{2}$	1500	70
High	1	1100	60
Center	0	700	50
Low	-1	300	40
Axial point	$-\sqrt{2}$	0	30

Table 8: Matrix of CCD experimental design using two variables.

Code		Original	
Rotational speed (rpm)	Temperature (°C)	Rotational speed (rpm)	Temperature (°C)
1	1	1100	60
1	-1	1100	40
-1	1	300	60
-1	-1	300	40
1.4	0	1500	50
-1.4	0	0	50
0	1.4	700	70
0	-1.4	700	30
0	0	700	50
0	0	700	50

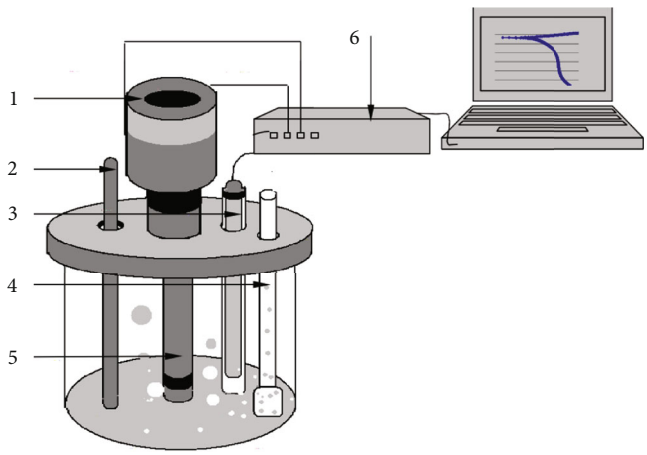

1- Rotator
2- Counter electrode
3- Reference electrode
4- Gas bubbler
5- Working electrode
6- Potentiostat

Figure 2: Electrochemical test for corrosion measurement [13].

2.4. Design of Experiment. Corrosion patterns can create a mathematical representation of the corrosion process using fundamental ideas from electrochemical reactions, which show exponential models [1]. Using these trends, a corrosion

Table 9: Experiment design of independent variable to study corrosion rate in nanocoolant.

Code		Original		Corr. rate (mm/y)		
Rotational	Temperature	Rotational	Temperature	Measured (y)	Predicted (ŷ)	y-ŷ
1	1	1100	60	4.837	4.914	-0.077
1	-1	1100	40	3.161	2.914	0.247
-1	1	300	60	1.163	1.398	-0.235
-1	-1	300	40	0.890	0.800	0.090
1.4	0	1500	50	4.475	4.493	-0.018
-1.4	0	0	50	0.394	0.552	-0.158
0	1.4	700	70	3.979	3.431	0.548
0	-1.4	700	30	1.225	1.612	-0.387
0	0	700	50	3.284	3.284	0.000
0	0	700	50	3.150	3.284	-0.134

Table 10: Experiment design of independent variable to study corrosion rate in the conventional coolant.

Code		Original		Corr. rate (mm/y)		
Rotational	Temperature	Rotational	Temperature	Measured (y)	Predicted (ŷ)	y-ŷ
1	1	1100	60	1.916	1.981	-0.065
1	-1	1100	40	0.879	0.956	-0.077
-1	1	300	60	0.723	0.766	-0.043
-1	-1	300	40	0.418	0.473	-0.055
1.4	0	1500	50	1.924	1.683	0.241
-1.4	0	0	50	0.406	0.495	-0.089
0	1.4	700	70	1.702	1.451	0.251
0	-1.4	700	30	0.430	0.528	-0.098
0	0	700	50	0.800	0.800	0.000
0	0	700	50	0.820	0.800	0.020

model was developed using a second-order regression in response surface methodology (RSM) technique.

The technique of design of experiment (DOE) is applied to identify important parameters and examine the potential impact of variables in experimental settings [10, 13]. Additionally, it is useful in minimizing potential errors and enhancing experimental efficiency. The outcomes obtained through the DOE approach are subject to analytical analysis and statistical validation. A central composite design (CCD) is chosen and applied to establish a corrosion rate model using temperature and rotational speed, as depicted in Tables 6 and 7. Table 8 presents the matrix of CCD, employing two independent variables to generate second-degree model regression formulas. A CCD was employed to examine the response pattern and establish the collective impact of these variables. To ensure that variables in the experiments vary within the same range, the values of variables should be in a coded form (Equation (1)). This coded value is also crucial in managing the results to align with a normal distribution pattern. The variables were coded using the following equation [13]:

$$X_{\text{code}} = \frac{2\left(x - x_{\text{high}}\right)}{x_{\text{high}} - x_{\text{low}}} + 1. \quad (1)$$

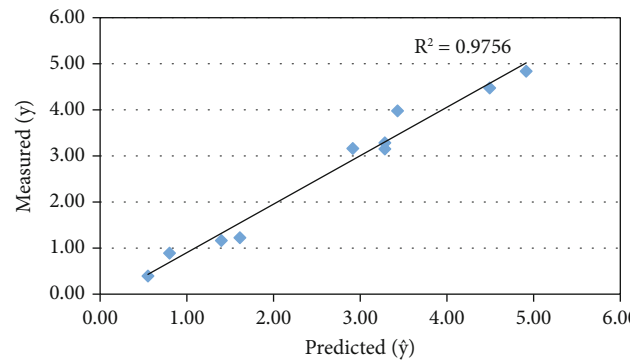

Figure 3: A relationship between measured and predicted values of the corrosion rate for nanocoolant.

2.4.1. Preparation of Specimen. The working electrodes were made of material of stainless steel (AISI 316). The specimens with a 16 mm diameter and a 10 mm thickness were used in the experiments. The specimen surfaces were ground and polished with 180, 320, and 600 grit SiC paper successively. And then, the samples were rinsed with methanol and dried with a dryer.

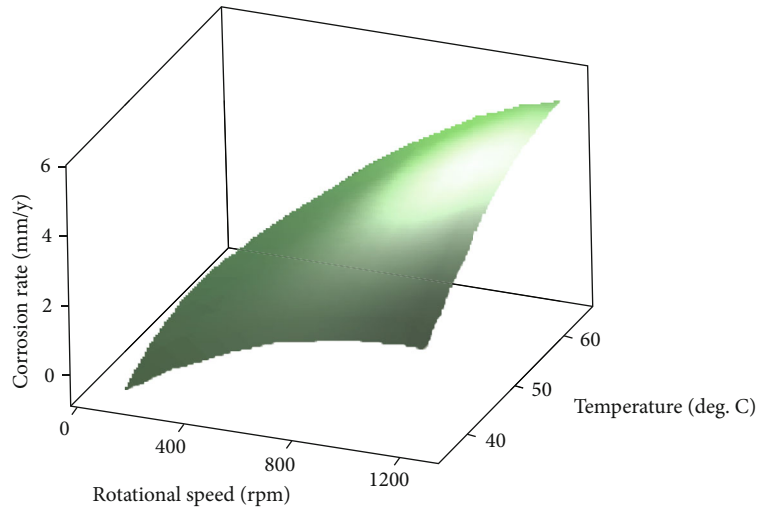

Figure 4: Surface plot of corrosion rate vs. temperature and rotational speed for nanocoolant.

2.5. Corrosion Experiments. The experiments were carried out in two distinct coolant types: traditional coolant and nanofluid, under stagnant (static test) and rotating conditions (dynamic test). The static tests were utilized to investigate corrosion behavior in a nonflowing solution. For these purposes, a three-electrode system (LPR method) was utilized. On the other hand, the dynamic tests were performed under various rotational speeds using a rotating cylinder electrode. The AISI 316 stainless steel specimens were positioned between PTFE washers, and an end cap was secured to the specimen holder's end. The cylindrical working electrodes were then attached to an electrode holder at the cell's center to facilitate rotation (Figure 2).

3. Results and Discussion

Tables 9 and 10 illustrate the impact of different temperature and flow conditions on corrosion rates, determined using the linear polarization resistance (LPR) technique. The experimental design employed the central composite design (CCD) to model corrosion behavior. From the CCD matrices, a regression model for corrosion rates was developed by fitting a second-order polynomial equation, which was analyzed using the least squares method. The constant parameter model was then calculated to derive a regression model representing the empirical relationship between the tested variables as expressed in Equations (2) and (3).

3.1. Parameter Estimates. Assuming the corrosion rate of the mechanical model adheres to a second-degree polynomial, it represents the most optimal fit. Consequently, by aligning this curve with the empirical data, a regression equation was derived using the encoded coefficients, as depicted in Equations (2) and (3) below.

Nanocoolant is as follows:

$$\text{Corrosion rate} = 1.41R + 0.65T - 0.39R^2 - 0.39T^2 + 0.35RT + 3.28. \quad (2)$$

Conventional coolant is as follows:

$$\text{Corrosion rate} = 0.42R + 0.33T + 0.15R^2 + 0.10T^2 + 0.18RT + 0.8000, \quad (3)$$

where the corrosion rate is measured in mm/year, R is the rotational speed (rpm), and T is the temperature (°C).

Figure 3 presents the relationship between measured and predicted data. From the figure, it can be seen that there is a strong interrelation between the model and the results of the experiment which is 97%.

3.2. Analysis and Interpretation of Response Surface

3.2.1. Combination Effect of Temperature and Rotational Speed on Corrosion Rate in Nanocoolant. The visualization of the RSM model enables the anticipation of the collective influence of rotation speed and temperature on the corrosion rate. Figure 4 shows the simultaneous effects of temperature and rotational speed on the corrosion rate. The graph reveals gradual effects on the corrosion rate with the combined impact of rotational speed and temperature. For instance, at a lower rotational speed (200 rpm), the temperature's influence leads to a corrosion rate rise of up to 1 mm/year. This trend persists across all temperature conditions. Notably, when the rotational speed reaches 1200 rpm and the temperature is 55°C, the corrosion rate escalates to 5 mm/year. This observation has shown the connection between heightened corrosion rates and elevated levels of rotational speed and temperature.

3.3. Analysis and Discussions for the Experimental Results. In Figure 3, the variations in corrosion rate at the various rotational speeds and temperatures are identified. The corrosion rate increases with the increase in temperature and rotational speed in both cases. According to Figure 3, the corrosion rate is minimally affected by temperature at lower rotation speeds. However, at higher rotation speeds, increasing temperature leads to a significant increase in corrosion

rate. These results align with previous research by references [9, 10, 13], which similarly found that higher temperatures tend to result in localized corrosion. This proves that the corrosion rate is highly influenced by the synergistic effects of temperature and rotational speed. Generally, higher temperatures expedite corrosion rates due to increased chemical activity [1, 10, 13].

In general, Figures 5–7 show that at higher temperatures, the corrosion rate tends to stabilize. This phenomenon can be attributed to the increased diffusion coefficient of species, which accelerates the formation of a protective film on the metal surface. Consequently, this film reduces the corrosion rate [13]. At higher temperatures, the access of oxygen into the metal is limited when a protective layer is formed. Although higher temperatures can accelerate corrosion, the decrease in oxygen solubility acts as a counterbalance. Rotational speed stands as an additional factor influencing the corrosion rate. The hydrodynamic conditions can enhance the movement of metal ions formed during metal dissolution from the electrode surface to the solution's bulk [27]. The increase in corrosion rate due to fluid velocity is related to heightened turbulence and mixing in the solution. High velocity accelerates corrosion by enhancing the transport of cathodic species toward the steel surface through turbulent flow [8, 9, 13]. Nonetheless, at higher rotation speeds (as indicated in Figure 6), there was a trend where the corrosion rate reduced. This phenomenon may be associated with the limiting current density mechanism at the cathode site [10].

3.4. Comparison of Nanocoolant and Conventional Coolant on Average Roughness Depth. Figure 5 illustrates a comparison of the effect of the erosion rate, represented by surface roughness, on the corrosion rate of stainless steel for a fluid with nanoparticles versus a conventional coolant. Experiments were conducted at a rotation speed of 1800 rpm. Results showed that the average roughness depth increased with temperature for both the nanocoolant and the conventional coolant. However, the erosion rate was consistently higher for the nanocoolant due to the mechanical force and friction during the experiment. This suggests that a synergistic effect of erosion and corrosion occurred, where solid particles of the nanofluids contributed to specimen damage.

3.5. The Comparative Effect of Rotation Speed and Temperature on Corrosion Rate between Nanocoolant and Conventional Coolant. In both nanocoolant and conventional coolant, the corrosion rate of stainless steel increased as the rotation speed increased (see Figure 6). The observed phenomenon can be attributed to the acceleration of electrochemical reaction transfer, resulting in both mass transfer reactions and hydrodynamic effects on the solution [13]. Increasing the rotational speed can additionally diminish the thickness of the solution's boundary layer adjacent to a metal surface. This decreased boundary layer thickness facilitates a faster corrosion process on the metal surface by enabling the dissolved species to act more rapidly [1, 9, 10]. The study also revealed that the corrosion rate of stainless steel increased when temperatures increased (Figure 7). One possible explanation for this is the acceleration of the

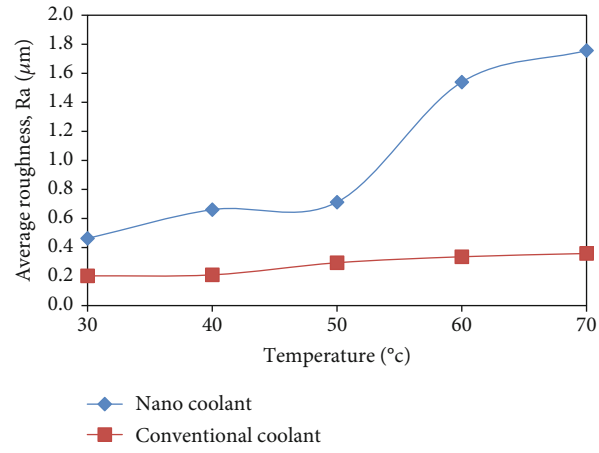

Figure 5: Average roughness versus temperature of nanocoolant and conventional coolant.

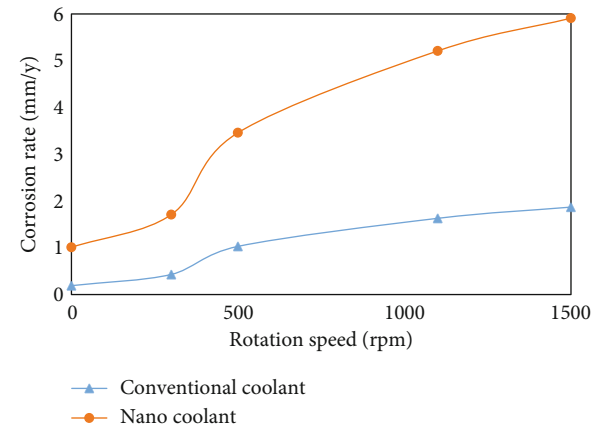

Figure 6: Effect of rotation speed on the corrosion rate of 316 stainless steel on nanocoolant and conventional coolant.

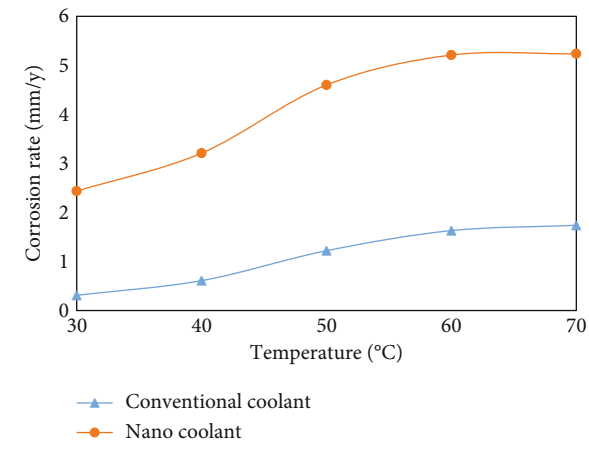

Figure 7: Effect of temperature on the corrosion rate of 316 stainless steel on nanocoolant and conventional coolant. Average roughness versus temperature of nanocoolant and conventional coolant.

cathodic reaction produced by hydrogen ions through the dissociation reaction and reduction in fluid coolant. It can be seen that a direct relationship between the temperature and the concentration of hydrogen evolution was observed [13].

4. Conclusions

This study found that when the experiment was conducted in static conditions, the corrosion rate of 316 stainless steel was higher in nanocoolant than in conventional coolant. The use of nanocoolant resulted in a higher corrosion rate compared to conventional coolant. The presence of suspended nanoparticles in the nanocoolant is believed to contribute to this effect by acting as an erosive medium. Although the presence of TiO_2 nanoparticles in the nanocoolant did have some effect on the erosion rate, the synergistic effect of erosion and corrosion was much more pronounced in flowing nanofluids. This can be attributed to mechanical wear, which damages the specimen's protective layer and exposes it to corrosive agents such as oxygen. Further research is needed to fully understand the underlying mechanisms and to identify strategies for mitigating these effects. The results indicate that the corrosion effects of nanocoolant should be considered when designing cooling systems.

Data Availability

The underlying data supporting the results of our study are available within the article itself.

Conflicts of Interest

The authors declare that they have no conflicting interests or personal relationships that could influence the research reported in this paper.

Acknowledgments

This work was supported by the Faculty of Engineering at Universiti Malaysia Pahang as funding for the final year project, with additional publication funding provided by the INTI International University.

References

[1] D. N. Veritas, "Recommended practice Rp O501 erosive wear in piping systems," *DNV Recommended Practice*, vol. 4, no. 2, pp. 1–43, 2007.

[2] J. A. Eastman, S. U. S. Choi, S. Li, W. Yu, and L. J. Thompson, "Anomalously increased effective thermal conductivities of ethylene glycol-based nanofluids containing copper nanoparticles," *Applied Physics Letters*, vol. 78, no. 6, pp. 718–720, 2001.

[3] T. Alisina, A. Sanam, and M. Pakshir, "Corrosion rate of carbon steel under synergistic effect of seawater parameters including pH, temperature, and salinity in turbulent conditions," *Corrosion Reviews*, vol. 16, 2013.

[4] A. Asgharpour, P. Zahedi, H. A. Khanouki, S. A. Shirazi, and B. S. McLaury, "Experimental investigation of solid particle erosion in successive elbows in gas dominated flows," *Journal of Fluids Engineering*, vol. 142, no. 6, article 061402, 2018.

[5] R. Asma, Y. P. Asmara, and C. I. Mokhtar, "Study on the effect of surface finish on corrosion of carbon steel in CO2 environment," *Journal of Applied Sciences*, vol. 11, no. 11, pp. 2053–2057, 2011.

[6] Y. P. Asmara, C. Ismail, L. G. Chui, and J. Halimi, "Predicting effects of corrosion erosion of high strength steel pipelines elbow on CO2-acetic acid (HAc) solution," *IOP Conference Series: Materials Science and Engineering*, vol. 114, article 012128, 2016.

[7] Y. P. Asmara, K. Siregar, T. Cionita, and J. Alias, "Electrochemical behaviour of high stress steel (AISI 4340) in CO_2 environments with the presence of H_2 gas," *Applied Mechanics and Materials*, vol. 695, pp. 98–101, 2014.

[8] Y. P. Asmara, Y. C. Wei, M. F. Ismail, and K. Yusuf, "Flow assisted erosion-corrosion of high speed steel (HSS) in nanofluid coolant," *Applied Mechanics and Materials*, vol. 695, pp. 143–146, 2014.

[9] Y. P. Asmara, A. Juliawati, A. Sulaiman, and Jamiluddin, "Mechanistic model of stress corrosion cracking (SCC) of carbon steel in acidic solution with the presence of H2S," *In IOP Conference Series: Materials Science and Engineering*, vol. 50, article 012072, 2013.

[10] Y. P. Asmara, K. Siregar, and Bachtiar, "Application of response surface methodology method in designing corrosion inhibitor," *IOP Conference Series: Materials Science and Engineering*, vol. 257, no. 1, article 012090, 2017.

[11] T. Hong and M. Nagumo, "Effect of surface roughness on early stages of pitting corrosion of type 301 stainless steel," *Corrosion Science*, vol. 39, no. 9, pp. 1665–1672, 1997.

[12] A. Stoilov and D. Northwood, "The relationship between surface roughness and corrosion," in *Proceedings of the ASME 2013 International Mechanical Engineering Congress and Exposition*, Volume 2B: Advanced Manufacturing, 2013.

[13] Y. P. Asmara, *A new approach in empirical modelling of CO_2 corrosion with the presence of HAc and H_2S, [Ph.D. thesis]*, Universti Teknologi Petronas, 2010.

[14] M. Hegde, M. Mroczkowska, J. Mohan et al., "Influence of physical and mechanical parameters on cavitation erosion and antifouling behaviour of multilayer silica-based hybrid sol–gel coatings on aluminium alloys," *Engineering*, vol. 4, no. 2, pp. 1393–1408, 2023.

[15] A. Toudehdehghan, J. W. Lim, K. E. Foo, M. I. N. Ma'arof, and J. Mathews, "A brief review of functionally graded materials," *MATEC Web Conferences*, vol. 131, p. 03010, 2017.

[16] C. M. H. Hagen, O. Ø. Hognestad, K. Knudsen, and K. Sørby, "The effect of surface roughness on corrosion resistance of machined and epoxy coated steel," *Progress in Organic Coatings*, vol. 130, pp. 17–23, 2019.

[17] K. Haugen, O. Kvernvold, A. Ronold, and R. Sandberg, "Sand erosion of wear resistant materials," in *8th international conference on erosion by liquid and solid impact*, Cambridge, 1994.

[18] H. Zhao, M. Yu, J. Liu, S. Li, B. Xue, and M. Liang, "Effect of surface roughness on corrosion resistance of sol-gel coatings on AA2024-T3 alloy," *Journal of the Electrochemical Society*, vol. 162, no. 14, pp. C718–C724, 2015.

[19] A. Ghadimi, R. Saidur, and H. S. C. Metselaar, "A review of nanofluid stability properties and characterization in stationary conditions," *International Journal of Heat and Mass Transfer*, vol. 54, no. 17-18, pp. 4051–4068, 2011.

[20] Z. Hanyang, G. Min, Z. Xingwen, W. Long, and W. Emori, "Corrosion behavior of 3A21 aluminum alloy in ethylene glycol solution under different atmospheres IOP Publishing Ltd," *Materials Research Express*, vol. 7, no. 2, 2020.

[21] K. Kwak and C. Kim, "Viscosity and thermal conductivity of copper oxide nanofluid dispersed in ethylene glycol," *Korea-Australia Rheology Journal*, vol. 17, no. 2, pp. 35–40, 2005.

[22] C. T. Yaw, S. P. Koh, M. Sandhya et al., "Heat transfer enhancement by hybrid nano additives—graphene nanoplatelets/cellulose nanocrystal for the automobile cooling system (radiator)," *Nanomaterials*, vol. 13, no. 5, p. 808, 2023.

[23] Q. Tao, F. Zhong, Y. Deng, Y. Wang, and C. Su, "A review of nanofluids as coolants for thermal management systems in fuel cell vehicles," *Nanomaterials*, vol. 13, no. 21, p. 2861, 2023.

[24] M. Ikeda, V. Ueda, A. Viloria, and Moralez, "Effects of flow velocity of 13Cr, super 13Cr and - duplex stainless steels," *Erosive Wear in Piping Systems*, vol. 4, no. 2, 2007.

[25] O. Kvernvold and R. Sandberg, *Production rate limits in two-phase flow systems–sand erosion in piping systems*, DNV Report. No, 1993.

[26] T. Lindheim, "Erosion performance of glass fiber reinforced plastics (GRP)," *International conference on composite materials in petroleum industry, IFP rencontres Scientifiques, energies nouvelles, November 3-4*, 1994.

[27] G. Ziskind, M. Fichman, and C. Gutfinger, "Particle behavior on surfaces subjected to external excitations," *Journal of Aerosol Science*, vol. 31, no. 6, pp. 703–719, 2000.

[28] Q. Mazumder, K. Ahmed, and S. Zhao, "Experimental investigation of solid particle erosion in S-bend," *Journal of Fluids Engineering-transactions of The Asme*, vol. 138, no. 4, article 044501, 2016.

[29] G. P. Tilly, "Erosion caused by impact of solid particles," *Treatise of Material Science and Technology*, vol. 13, 1979.

[30] N. Molina, M. Walczak, M. Kalbarczyk, and D. J. Celentano, "Erosion under turbulent slurry flow: effect of particle size in determining impact velocity and wear correlation by inverse analysis," *Wear*, vol. 474-475, article 203651, 2021.

[31] L. Wang, Z. Zhang, L. Zhang, and Y. Chen, "Corrosion resistance of carbon steel in nanofluids containing graphene nanoparticles," *Corrosion Science*, vol. 148, pp. 76–83, 2019.

[32] J. Li, M. Li, X. Li, S. Zhou, and T. Zhang, "Erosion-corrosion behavior of stainless steel in nanocoolants containing silica nanoparticles," *Wear*, vol. 469, no. 1, article 203316, 2020.

[33] Q. Zhang, X. Wang, Y. Chen, and Y. Cheng, "Molecular dynamics simulation of corrosion behaviors of steel in nanocoolants," *Journal of Materials Science & Technology*, vol. 80, pp. 252–262, 2021.